



Phylogeny of the *Stipa* and implications for grassland evolution in China: based on biogeographic evidence

1 **Qing Zhang^{1*}, Junjun Chen¹, Yong Ding²**

2 ¹ School of Ecology and Environment, Inner Mongolia University, Hohhot, 010021,

3 China

4 ² Grassland Research Institute of Chinese Academy of Agricultural Sciences, Hohhot,

5 010010, China;

6 * Corresponding author. Email: qzhang82@163.com

7

8 **Abstract**

9 The evolution of Chinese grassland is a still an important question biogeography. In this study, the
10 phylogeny of 20 *Stipa* species (extensively distributed in Chinese grassland) was established to
11 explore the origin and dispersal routes of Chinese grassland. It showed that *Stipa* species
12 originated at 28 MaBP and they started to differentiate in central Inner Mongolia at 22 MaBP.
13 Then, *Stipa* species expanded along four routes: (1) they expanded from central Mongolia to the
14 Qilian Mountains, Qinghai, and western Tibet at 16 MaBP. They then gradually expanded from
15 western to eastern Tibet from 11-6 MaBP. (2) At 12 MaBP, they expanded from central Inner
16 Mongolia to the Helan Mountains. (3) At 8 MaBP, they expanded from central Inner Mongolia to
17 the Xinjiang area. (4) At 4 MaBP, they expanded from central to eastern Inner Mongolia.
18 Therefore, we could deduce the formation order of Chinese grasslands: central Inner Mongolia >
19 Qilian Mountains > Qinghai > western Tibet > Helan Mountains > Xinjiang > central Tibet >
20 eastern Tibet > eastern Inner Mongolia. We highlight the importance of the uplift of the
21 Qinghai-Tibet Plateau and paleoclimate changes in triggering the origin and evolution of *Stipa*
22 species and Chinese grasslands.

23 **Keywords:** uplift of the Qinghai-Tibet Plateau; paleoclimate; explosive radiation;
24 phylogeny



25

26 **1 Introduction**

27 Different regions on earth harbor distinct biological species even though their
28 environment are the same, indicating that the distribution of organisms not only is
29 driven by contemporary ecological factors but may also be closely associated with
30 historical factors (e.g., geological evolutionary history and population evolutionary
31 history) (Medail and Diadema, 2009; Ordonez and Svenning, 2015; Santos et al.,
32 2017). Based on molecular clocks, the genetic information of existing species could
33 be used to explore the biogeographic processes including the origin, divergence,
34 expansion, and isolation of organisms at the molecular level during all important
35 geological history events. In addition, the time of divergence between closely related
36 species could be basically confirmed (Tedesco et al., 2017; Voskamp et al., 2017;
37 Wang et al., 2017a).

38 Grasslands are an important component of the global ecosystem and provide
39 significant ecosystem functioning and service.. One sixth total land area is covered by
40 grassland (Scurlock and Hall, 1998). The Chinese grasslands, starting from the
41 Northeast China Plain, Inner Mongolian Plateau, Ordos Plateau, and Loess Plateau to
42 the southern margin of the Qinghai-Tibet Plateau, are major part of the Eurasian
43 Steppe, which is the world's largest grassland (Addison and Greiner, 2016; Wu et al.,
44 2015). The Chinese grasslands are of great interests in ecological studies, including
45 grassland biodiversity (Buergi et al., 2015; Yuan et al., 2016), community assembly
46 (Li and Wu, 2016; Niu et al., 2016), stoichiometry (Wang et al., 2017b), and
47 ecosystem function (Jing et al., 2015; Mao et al., 2017). Meanwhile, a few studies
48 have also discussed the origin and dispersal routes of Chinese grassland genus (Favre
49 et al., 2016; Luo et al., 2016). However, the formation and evolutionary processes of
50 Chinese grasslands are still rarely studied.

51 According to paleogeographical climate change, Chinese grasslands might first
52 emerge in the late of the Tertiary Period because of the global cooling and
53 aridification (Wu et al., 2015). In addition, Meang and McKenna (1998) found that
54 perissodactyl-dominant faunas of the Eocene were abruptly replaced by



55 rodent/lagomorph-dominant faunas of the Oligocene in Mongolia Plateau at 33 MaBP,
56 similar to the European *Grande Coupure*. And they think the turnovers were mainly
57 driven by global climatic shifts and prominent biotic reorganization from forest to
58 grassland. Based on the evidence of sporopollen, more studies focused on vegetation
59 shift and climate change in steppe area of China during the mid-late Holocene
60 (Mischke et al., 2016; Shen et al., 2008). These studies are of great importance for
61 revealing the origin and evolution of Chinese grasslands. However, they were mainly
62 based on a certain history period, and did not explain the expansion routes of Chinese
63 grasslands. We need more direct evidence to obtain a comprehensive and continuous
64 history of grassland evolution. Based on currently molecular information, which
65 providing more accurate and direct evidence for the evolutionary process,
66 biogeography can be used to deduce the origin and expansion routes of Chinese
67 grasslands and to explore the effects of important geological historical events (Favre
68 et al., 2016; Ferreira et al., 2017).

69 Although Chinese grasslands is vast and covers different vegetation types, *Stipa*
70 species are dominant through the whole Eurasian steppe, including Chinese
71 grasslands (Durka et al., 2013; Hamasha et al., 2012). Because of differences in
72 climate, *Stipa* species show obvious zonal distribution characteristics in Chinese
73 grasslands. *Stipa baicalensis*, *Stipa grandis*, and *Stipa krylovii* are constructive
74 species in the typical grasslands; *Stipa tianschanica* and *Stipa glareosa* are distributed
75 extensively in the desert steppe; and *Stipa purpurea* has a very extensive distribution
76 in alpine steppes. In addition, *Stipa basiplumosa* and *Stipa subsessiliflora* are also
77 distributed in the high mountains of desert areas (Durka et al., 2013; Wu et al., 2015).
78 Therefore, *Stipa* species play very important roles in the formation of Chinese
79 grasslands. The evolutionary processes of Chinese grasslands are closely related to the
80 evolution of *Stipa* species. Studies on the history of origin, divergence and expansion
81 routes of *Stipa* species are an excellent indicator to reveal the evolution of Chinese
82 grasslands. Therefore, in this study, *Stipa* species that were distributed extensively in
83 different grassland areas including Inner Mongolia, Qinghai, Tibet, and Xinjiang were
84 collected. The four gene fragments of chloroplasts, *matk*, *rbcl*, *trnh-psba*, and *trnl-f*,



85 were selected to estimate the divergence time tree of *Stipa* species using BEAST
86 (Bayesian evolutionary analysis by sampling trees). In addition, the origin, divergence
87 and expansion routes of *Stipa* species were reconstructed based on RASP
88 (Reconstruct Ancestral State in Phylogenies). Finally, the origin and evolutionary
89 processes of Chinese grasslands were deduced and the effects of paleoclimate and
90 geological historical events were further explored.

91

92 **2 Materials and Methods**

93 **2.1 Materials**

94 This study contained 20 species of *Stipa* species collected from seven different
95 grasslands area (Fig 1, Table 1). *Helictotrichon schellianum*, *Achnatherum splendens*,
96 and *Ptilagrostis pelliottii*, which are closely related to *Stipa* species, were used as the
97 outgroup (Hamasha et al., 2012). Considering there is certain hybridization between
98 *Stipa* species (Gonzalo et al., 2012), nuclear-derived markers were not employed, and
99 the four gene fragments of chlorophyll, *matk*, *rbcl*, *trnh-psba*, and *trnl-f*, were used for
100 analyses.

101 **2.2 Methods**

102 **2.2.1 Total DNA extraction, PCR amplification, and sequencing**

103 This study performed total DNA extraction using the Plant Genome Extraction
104 Kit (Tiangen Biotech, Beijing, China). DNA samples were diluted to 30 ng/μL for
105 future use (Ramirez et al., 2017). The four selected gene fragments were amplified by
106 PCR. The universal primers were acquired from previous studies (Durka et al., 2013;
107 Hamasha et al., 2012; Ren et al., 2011). The PCR reaction volume was 50 μL;
108 specifically, 2 μL of DNA template, 2 μL each of upstream and downstream primers,
109 25 μL of 2×PfuUltra Master Mix, and 24 μL ddH₂O were combined (Lu et al., 2013).
110 The *matk* gene amplification was carried out using the following procedure:
111 pre-denaturation at 94 °C for 5 min; 30 cycles of denaturation at 94 °C for 30 s,
112 annealing at 40 °C for 30 s, and extension at 72 °C for 1 min; and a final extension at
113 72 °C for 10 min. The same amplification procedure was used for the *trnh-psba*
114 sequence. For the amplification of *trnl-f* and *rbcl*, the annealing temperatures were



115 changed to 57 °C and 52 °C, respectively, and the other conditions remained
116 unchanged. The amplification products were subjected to 1% agarose gel
117 electrophoresis and sent to the Beijing Genomics Institute for sequencing when the
118 samples were ready.

119 2.2.2 Sequence comparison

120 The molecular data obtained from sequencing were assembled using BioEdit and
121 compared using ClustalW. The sequence length, conserved sites, and GC content were
122 analyzed using MEGA5.0. These sequence data have been submitted to the GenBank
123 databases under accession number (see appendices).

124 2.2.3 Divergence time tree construction using BEAST

125 The combined sequences of the four gene fragments were used for divergence
126 time tree construction. Therefore, incongruence length difference (ILD) analysis
127 (heterogeneity test) on the combined gene fragments was required. This analysis was
128 performed using PAUP (Mathews and Rosenberger, 2008). The results showed that
129 $P > 0.01$, indicating that these fragments did not have an obvious conflict and could be
130 used for combined analysis (Rix and Harvey, 2012). In addition, the model selection
131 software jModeltest (Posada, 2008) was used to calculate the screening of the optimal
132 model; the selected model was GTR+G. Because there was no suitable *Stipa* fossil or
133 gene fragment evolution rate, the average evolution rate of chloroplast gene of
134 herbaceous plants (3.46×10^{-9} s/y) was used to calculate the divergence times. First,
135 the model was operated for 100 million generations in BEAST (Drummond and
136 Rambaut, 2007). After the operation was finished, TRACER V1.6 (Rambaut and
137 Drummond, 2013) was used to look up the ESS value. If the ESS value was larger
138 than 200, the result was considered reliable. Finally, the final divergence time tree was
139 checked in FigTree (Rambaut, 2009), which provided the divergence time for *Stipa*
140 species.

141 2.2.4 Reconstruction of historical distribution areas of *Stipa* species based on RASP

142 This study used the RASP software to deduce the ancestral distribution areas of
143 internal nodes in the tree. The Chinese grasslands were divided into seven sections:
144 (A) eastern Inner Mongolia, (B) central Inner Mongolia, (C) the Helan Mountains, (D)



145 the Qilian Mountains, (E) Qinghai, (F) Tibet, and (G) Xinjiang. The S-DIVA analysis
146 used all 100 trees and combined trees in the Bayesian collection. A total of 2500
147 random trees were selected in the analysis. The maximum number of distributions in
148 each distribution area was set as two, and the remaining settings were the default ones
149 (Lu et al., 2013).

150 **3 Results**

151 **3.1 Results of sequence feature analysis**

152 The combined analyses of the four gene fragments showed that the length of the
153 combined gene fragments was 4093 bp; 2988 bp were conserved sites, 1102 bp were
154 mutation sites, 227 bp were parsimony-informative sites, and 847 bp were single
155 information sites. The percentage of G+C in the whole sequence was 37.5%, which
156 was much lower than the A+T content.

157 **3.2 Divergence time of *Stipa* species**

158 The results showed that the divergence time between *Stipa* species and the
159 outgroup (*Achnatherum splendens*, *Helictotrichon schellianum*, and *Ptilagrostis*
160 *pelliotii*) was 28.42 MaBP (Oligocene period) based on the joint matrix estimate (Fig.
161 2). The divergence time of *Stipa* species was 22.10 MaBP (early Miocene period).
162 There is a explosive rapid radiation of *Stipa* species around 6.0 MaBP (Fig.2).

163 **3.3 Analysis of reconstruction of ancestral distribution areas of *Stipa* species** 164 **using RASP**

165 RASP analyses showed that *Stipa* species originated and diverged from the
166 outgroup at 28 MaBP (Fig. 3). At node ① (22 MaBP), *Stipa* species began to
167 differentiate in central Inner Mongolia. The current distribution pattern of *Stipa*
168 species was formed through 16 expansions and 13 isolated divergences, and the
169 process was more complicated. At node ② (18 MaBP), *Stipa* species first expanded
170 to near the Qilian Mountains, Qinghai. Subsequently, at node ③ (13-11 MaBP),
171 there was a stronger interaction between the top and bottom of mountains in the
172 Qilian Mountains and other areas in Qinghai. At node ④ (16 MaBP), *Stipa* species
173 had already expanded from Qinghai to Tibet; however, no large-area expansion



174 occurred immediately. Instead, at node ⑥ (11 MaBP-6 MaBP), *Stipa* species had an
175 east to west expansion in Tibet. At node ⑤ (12 MaBP), *Stipa* species expanded
176 along another route from central Inner Mongolia to the Helan Mountains. At node ⑦
177 (8 MaBP), the expansion route was from central Inner Mongolia to Xinjiang. Finally,
178 at node ⑧ (4 MaBP), the expansion route of the *Stipa* species was from central to
179 eastern Inner Mongolia.

180 **3.4 Important influences of paleoclimate and geological historical events on the** 181 **evolutionary history of *Stipa* species**

182 Fig 4 shows that *Stipa* species underwent three larger expansion and isolation
183 events. The first larger expansion occurred around 22 MaBP, the second larger
184 expansion occurred approximately 19-16 MaBP, and the third larger expansion
185 occurred around 12-10 MaBP. The peak values of isolation events and expansion
186 events of *Stipa* species were basically matched. The peak values had certain
187 relationships with the second uplift of the Qinghai-Tibet Plateau and paleoclimate
188 change, including East Asian monsoon formation and polar ice cap development.

189 **4 Discussion**

190 **4.1 Origin and differentiation of *Stipa* species**

191 Mountain building may trigger the origin and radiation of species by providing
192 vacant niches and habitat alternatives within a short distance (Favre et al., 2016;
193 Hoorn et al., 2013; Sun et al., 2012), for example in Andes (Hughes and Atchison,
194 2015), Himalaya-Hengduan Mountains (Luo et al., 2016) and uplift of the
195 Qinghai-Tibet Plateau (Sun et al., 2012). During the second (23-15 MaBP) and the
196 third (since 8 MaBP) uplift periods of the Qinghai-Tibet Plateau, many species groups,
197 including *Nannoglottis* (Liu et al., 2002), Chinese sisorid catfishes (Guo et al., 2006),
198 *Rheum* (Sun et al., 2012) and *Gentiana* (Favre et al., 2016). Therefore, the uplift of
199 the Qinghai-Tibet Plateau plays important role in the origin and divergence of many
200 species.

201 In this study, the results showed that *Stipa* species differentiated from the
202 outgroup and originated at 28 MaBP and began to differentiate at 22 MaBP in central
203 Inner Mongolia (Fig.3b). It is consistent with a previous study showing that *Stipa*



204 species were at least originated in the Miocene or Pliocene through fossil evidence in
205 North American (Thomasson, 1978). During this period, Himalayan movement had
206 already uplifted the Qinghai-Tibet Plateau to the height above 2000 m that had a
207 critical function in the formation of monsoon circulation (Molnar et al., 1993;
208 Tapponnier et al., 2001). With the continuous uplift and expansion of the plateau,
209 summer sea surface pressure on the Asian continent increased continuously. With the
210 presence of a monsoon climate, the humid climate that used to penetrate from Inner
211 Mongolia to northern Xinjiang no longer existed. This area became particularly arid,
212 which provided possibilities for the origin and first expansion of *Stipa* species.

213 Around 6.0 MaBP, there is a dichotomous relationship among these *Stipa* species,
214 and the internodes are consistently short relative to the average tip nodes (Fig.2).
215 These two results both provide clear indications of explosive rapid radiation in the
216 past (Hughes and Atchison, 2015; Sun et al., 2012). We speculate that this is the
217 results of the third uplift of the Qinghai-Tibet Plateau occurred during the 9-2.61
218 MaBP period (Molnar et al., 1993; Tapponnier et al., 2001). There may be two major
219 speciation mechanisms that caused the explosive rapid radiation of *Stipa* species at
220 that time. On one hand, the first speciation mechanism may be allopatric speciation
221 (Boucher et al., 2016). Due to the crumpling effect of the uplift of the Qinghai-Tibet
222 Plateau, the Tian Shan, Qilian, Altyn Tagh, and Kunlun Mountains all had a
223 large-scale elevation of fault blocks, and many areas that were already elevated
224 became medium-height mountains with around 4000 m height (Tapponnier et al.,
225 2001). During this period, geographic isolation was great obvious. As long as there
226 was obvious geographic isolation, species groups were divided into several small
227 species groups; because there was no continuous gene flow, different new species
228 would be generated (Lee and Lin, 2012; Tedesco et al., 2017). On the other hand, for
229 the area without obvious geographic isolation, such as the Inner Mongolian plateau,
230 we considered ecological speciation occurred in the presence of gene flow (Shafer and
231 Wolf, 2013). The uplift of the Qinghai-Tibet Plateau would have caused larger climate
232 fluctuations in Inner Mongolia Plateau (Tapponnier et al., 2001), thus gradually
233 generated different small geographic environments. These different small geographic



234 environments would cause species to occupy different ecological niches, resulting in
235 natural or sexual selection, which would have caused individuals of the ancestral
236 species group to undergo phenotype divergence to generate new species (Greve et al.,
237 2017; Shafer and Wolf, 2013). Therefore, the explosive rapid radiation of *Stipa*
238 species around 6.0 MaBP was the result of with and without gene flow driven by
239 geographic isolation and climate changes in different region. In addition, analysis of
240 their molecular characteristics showed that the G+C content accounted for 37.5% of
241 the total sequence length, which was much lower than the A+T content. A and T are
242 connected and expanded by two hydrogen bonds; therefore, they are more prone to
243 mutations than G and C (Lee et al., 2016). In addition to external environmental
244 factors, the molecular characteristics of *Stipa* species also made the occurrence of
245 rapid divergence possible.

246 **4.2 Influence of the Qinghai-Tibet Plateau uplifts and paleoclimate changes on** 247 **the origin and evolution of the grasslands**

248 During the developmental process of the whole geological history, various
249 geological history events continuously occur such as large tectonic movements, the
250 rise and fall of sea levels, magmatic activities, and volcanic eruptions. Climate
251 changes on earth are closely associated with these geological history events, whereas
252 the development of the biosphere is directly influenced by climate and terrain changes
253 (Guo et al., 2002; Molnar et al., 2010). In China, one of the geological history events
254 that had great influences on the biosphere were several larger uplift events of the
255 Qinghai-Tibet Plateau. After the collision between the Indian and European continents,
256 the Qinghai-Tibet area entered into a whole new developmental stage consisting of
257 mainly orogenic, fault, and magmatic activities (Tapponnier et al., 2001). There were
258 three main stages of uplift. The first stage occurred before 30 MaBP (Turner et al.,
259 1993), the second stage occurred from 23-15 MaBP, and the third stage occurred at 8
260 MaBP (Molnar et al., 1993). The uplift of the Qinghai-Tibet Plateau caused dramatic
261 climate changes on earth at that time, and the climate became dry and cold; these
262 changes were conducive to the origin and evolution of grasslands (Turner et al., 1993;
263 Wu et al., 2015).



264 Stipa species started to differentiate at 22 MaBP in central Inner Mongolia;
265 therefore, during the same period, this area already had a preliminary grassland
266 landscape. This grassland vegetation structure was also consistent with
267 rodent/lagomorph-dominant mammal faunas of the Oligocene in Mongolia Plateau
268 based on fossil evidence (Meng and McKenna, 1998). Afterward, when the expansion
269 of Stipa species occurred at 16 MaBP, grassland landscapes also emerged successively
270 in the Qilian Mountains, Qinghai, and western Tibet areas. The major event of
271 geological history at this stage was the second uplift of the Qinghai-Tibet Plateau. In
272 addition, factors such as the expansion of rifts in the Asian marginal sea and the
273 partial shrinkage and disappearance of the eastern extension of the Neo-Tethys Ocean
274 in Central Asia all resulted in the formation of the Neogene monsoon climate (Huang
275 et al., 2003; Wang et al., 2003). After it developed at 22 MaBP, the monsoon climate
276 continuously strengthened and became strongest at 16 MaBP. The strengthening of the
277 monsoon climate and aridification of the inland areas were synchronous, thereby
278 causing the further expansion of the arid areas in northwestern China. These events all
279 provided appropriate environmental conditions for the formation and expansion of the
280 grasslands (Guo et al., 2002; Wang et al., 2008). The late Miocene period in
281 geological history occurred approximately 12 MaBP. During this period, the Asian,
282 and even the global, environment also underwent significant changes. The Arctic area
283 had a large amount of ice rafts, the polar ice cap developed further, the climate
284 became drier and colder, an outbreak of C₄ plants occurred, and C₃ plants decreased
285 rapidly (Cerling et al., 1997). Based on these events, central Tibet and the ancient
286 Helan Mountains in Inner Mongolia also exhibited grassland landscapes. During the
287 period of 9-2.61 MaBP, the third uplift of the Qinghai-Tibet Plateau occurred. The
288 uplift of the Qilian Mountains, Tian Shan Mountains, Altyn Tagh Mountains, and
289 Kunlun Mountains made the inland areas more arid (Molnar et al., 1993). During this
290 period, western Tibet, Xinjiang, and eastern Inner Mongolia also successively
291 exhibited grassland landscapes. The uplift of the Qinghai-Tibet Plateau and changes in
292 paleoclimate jointly promoted the origin of grasslands.

293 **5 Conclusion**



294 In summary, *Stipa* species originated at 28 MaBP and they started to differentiate
295 in central Inner Mongolia at 22 MaBP. Then, *Stipa* species expanded along four routes.
296 Based on the expansion route of *Stipa* species, we deduced that the Chinese
297 grasslands formed in the following order: central Inner Mongolia > Qilian Mountains >
298 Qinghai > western Tibet > Helan Mountains > Xinjiang > central Tibet > eastern
299 Tibet > eastern Inner Mongolia. In addition, the origin and evolution of *Stipa* species
300 and Chinese grasslands were accompanied by the uplift of the Qinghai-Tibet Plateau
301 and paleoclimate change.

302 **6 Author contributions**

303 Q.Z. conceived the ideas. Q.Z. and J.C. complied the experiment and ran further
304 data analysis. Q.Z., C.L. and Y.D. collected study material. Q.Z. and J.C. led the
305 writing.

306 **7 Conflict of Interest Statement**

307 The authors declare that the research was conducted in the absence of any
308 commercial or financial relationships that could be construed as a potential conflict of
309 interest.

310 **8 Acknowledgements:**

311 We are grateful to professor Frank Yonghong Li and Morigen, for proposing
312 some valuable suggestions in experimental design. We also grateful professor Cunzhu
313 Liang for collected some study material. This study was supported by the National
314 Natural Science Foundation of China (31560180) and China Postdoctoral Science
315 Foundation.

316

317 **References**

- 318 Addison, J. and Greiner, R.: Applying the social-ecological systems framework to the evaluation and
319 design of payment for ecosystem service schemes in the Eurasian steppe, *Biodivers. Conserv.*, 25,
320 2421-2440, 2016.
- 321 Boucher, F. C., Zimmermann, N. E., and Conti, E.: Allopatric speciation with little niche divergence is
322 common among alpine Primulaceae, *J. Biogeogr.*, 43, 591-602, 2016.
- 323 Buergi, M., Li, L., and Kizos, T.: Exploring links between culture and biodiversity: studying land use
324 intensity from the plot to the landscape level, *Biodivers. Conserv.*, 24, 3285-3303, 2015.
- 325 Cerling, T. E., Harris, J. M., Macfadden, B. J., Leakey, M. G., Quade, J., Eisenmann, V., and Ehleringer,



- 326 J. R.: Global vegetation change through the Miocene/Pliocene boundary, *Nature* (London), 389,
327 153-158, 1997.
- 328 Drummond, A. J. and Rambaut, A.: BEAST: Bayesian evolutionary analysis by sampling trees, *BMC*
329 *Evol. Biol.*, 7, 2007.
- 330 Durka, W., Nossol, C., Welk, E., Ruprecht, E., Wagner, V., Wesche, K., and Hensen, I.: Extreme genetic
331 depauperation and differentiation of both populations and species in Eurasian feather grasses (*Stipa*),
332 *Plant Syst. Evol.*, 299, 259-269, 2013.
- 333 Favre, A., Michalak, I., Chen, C. H., Wang, J. C., Pringle, J. S., Matuszak, S., Sun, H., Yuan, Y. M.,
334 Struwe, L., and Muellner-Riehl, A. N.: Out-of-Tibet: the spatio-temporal evolution of *Gentiana*
335 (*Gentianaceae*), *J. Biogeogr.*, 43, 1967-1978, 2016.
- 336 Ferreira, M., Aleixo, A., Ribas, C. C., and Santos, M. P. D.: Biogeography of the Neotropical genus
337 *Malacoptila* (Aves: *Bucconidae*): the influence of the Andean orogeny, Amazonian drainage evolution
338 and palaeoclimate, *J. Biogeogr.*, 44, 748-759, 2017.
- 339 Gonzalo, R., Aedo, C., and García, M. Á.: Two New Combinations in *Stipa* sect. *Smirnovia* (*Poaceae*),
340 *Ann. Bot. Fenn.*, 48, 159-162, 2012.
- 341 Greve, C., Haase, M., Hutterer, R., Rödder, D., Ihlow, F., and Misof, B.: Snails in the desert: Species
342 diversification of *Theba* (*Gastropoda: Helicidae*) along the Atlantic coast of NW Africa, *Ecology and*
343 *Evolution*, 2017.
- 344 Guo, X. G., He, S. P., and Zhang, Y. G.: Phylogeny and biogeography of Chinese sisorid catfishes
345 re-examined using mitochondrial cytochrome b and 16S rRNA gene sequences (vol 35, pg 344, 2005),
346 *Mol. Phylogen. Evol.*, 38, 291-291, 2006.
- 347 Guo, Z. T., Ruddiman, W. F., Hao, Q. Z., Wu, H. B., Qiao, Y. S., Zhu, R. X., Peng, S. Z., Wei, J. J.,
348 Yuan, B. Y., and Liu, T. S.: Onset of Asian desertification by 22 Myr ago inferred from loess deposits in
349 China, *Nature*, 416, 159-163, 2002.
- 350 Hamasha, H. R., von Hagen, K. B., and Roeser, M.: *Stipa* (*Poaceae*) and allies in the Old World:
351 molecular phylogenetics realigns genus circumscription and gives evidence on the origin of American
352 and Australian lineages, *Plant Syst. Evol.*, 298, 351-367, 2012.
- 353 Hoorn, C., Mosbrugger, V., Mulch, A., and Antonelli, A.: Biodiversity from Mountain Building, *Nature*
354 *Geoscience*, 6, 154-154, 2013.
- 355 Huang, R. H., Zhou, L. T., and Chen, W.: The progresses of recent studies on the variabilities of the
356 East Asian monsoon and their causes, *Advances in Atmospheric Sciences*, 20, 55-69, 2003.
- 357 Hughes, C. E. and Atchison, G. W.: The ubiquity of alpine plant radiations: from the Andes to the
358 Hengduan Mountains, *New Phytol.*, 207, 275-282, 2015.
- 359 Jing, X., Sanders, N. J., Shi, Y., Chu, H., Classen, A. T., Zhao, K., Chen, L., Shi, Y., Jiang, Y., and He,
360 J.-S.: The links between ecosystem multifunctionality and above- and belowground biodiversity are
361 mediated by climate, *Nature Communications*, 6, 2015.
- 362 Lee, A.-W., Hsu, C.-C., Liu, Y.-Z., Wei, P.-L., and Chen, J.-K.: Supermolecules of
363 poly(*N*-isopropylacrylamide) complexing Herring sperm DNA with bio-multiple hydrogen bonding,
364 *Colloids and Surfaces B-Biointerfaces*, 148, 422-430, 2016.
- 365 Lee, Y.-H. and Lin, C.-P.: Pleistocene speciation with and without gene flow in *Euphaea* damselflies of
366 subtropical and tropical East Asian islands, *Mol. Ecol.*, 21, 3739-3756, 2012.
- 367 Li, S. W. and Wu, J. S.: Community assembly and functional leaf traits mediate precipitation use
368 efficiency of alpine grasslands along environmental gradients on the Tibetan Plateau, *PeerJ*, 4, 2016.
- 369 Liu, J. Q., Gao, T. G., Chen, Z. D., and Lu, A. M.: Molecular phylogeny and biogeography of the



- 370 Qinghai-Tibet Plateau endemic *Nannoglottis* (Asteraceae), *Mol. Phylogen. Evol.*, 23, 307-325, 2002.
- 371 Lu, L., Wang, W., Chen, Z., and Wen, J.: Phylogeny of the non-monophyletic *Cayratia* Juss. (Vitaceae)
372 and implications for character evolution and biogeography, *Mol. Phylogen. Evol.*, 68, 502-515, 2013.
- 373 Luo, D., Yue, J. P., Sun, W. G., Xu, B., Li, Z. M., Comes, H. P., and Sun, H.: Evolutionary history of
374 the subnival flora of the Himalaya-Hengduan Mountains: first insights from comparative
375 phylogeography of four perennial herbs, *J. Biogeogr.*, 43, 31-43, 2016.
- 376 Mao, W., Felton, A. J., and Zhang, T.: Linking Changes to Intraspecific Trait Diversity to Community
377 Functional Diversity and Biomass in Response to Snow and Nitrogen Addition Within an Inner
378 Mongolian Grassland, *Frontiers in Plant Science*, 8, 2017.
- 379 Matthews, L. J. and Rosenberger, A. L.: Taxon Combinations, Parsimony Analysis (PAUP*), and the
380 Taxonomy of the Yellow-Tailed Woolly Monkey, *Lagothrix flavicauda*, *Am. J. Phys. Anthropol.*, 137,
381 245-255, 2008.
- 382 Medail, F. and Diadema, K.: Glacial refugia influence plant diversity patterns in the Mediterranean
383 Basin, *J. Biogeogr.*, 36, 1333-1345, 2009.
- 384 Meng, J. and McKenna, M. C.: Faunal turnovers of Palaeogene mammals from the Mongolian plateau,
385 *Nature*, 394, 364-367, 1998.
- 386 Mischke, S., Lai, Z., Long, H., and Tian, F.: Holocene climate and landscape change in the northeastern
387 Tibetan Plateau foreland inferred from the Zhuyeze Lake record, *Holocene*, 26, 643-654, 2016.
- 388 Molnar, P., Boos, W. R., and Battisti, D. S.: Orographic Controls on Climate and Paleoclimate of Asia:
389 Thermal and Mechanical Roles for the Tibetan Plateau. In: *Annual Review of Earth and Planetary
390 Sciences*, Vol 38, Jeanloz, R. and Freeman, K. H. (Eds.), *Annual Review of Earth and Planetary
391 Sciences*, 2010.
- 392 Molnar, P., England, P., and Martinod, J.: Mantle dynamics, uplift of the Tibetan Plateau, and the Indian
393 Monsoon, *Rev. Geophys.*, 31, 357-396, 1993.
- 394 Niu, K., He, J.-S., Zhang, S., and Lechowicz, M. J.: Grazing increases functional richness but not
395 functional divergence in Tibetan alpine meadow plant communities, *Biodivers. Conserv.*, 25,
396 2441-2452, 2016.
- 397 Ordonez, A. and Svenning, J.-C.: Geographic patterns in functional diversity deficits are linked to
398 glacial-interglacial climate stability and accessibility, *Global Ecol. Biogeogr.*, 24, 826-837, 2015.
- 399 Posada, D.: jModelTest: Phylogenetic model averaging, *Mol. Biol. Evol.*, 25, 1253-1256, 2008.
- 400 Rambaut, A.: FigTree v1.3.1. 2006-2009, 2009.
- 401 Rambaut, A. and Drummond, A. J.: Tracer V1.6, 2013.
- 402 Ramirez, J. L., Birindelli, J. L. O., and Galetti, P. M., Jr.: A new genus of Anostomidae (Ostariophysi:
403 Characiformes): Diversity, phylogeny and biogeography based on cytogenetic, molecular and
404 morphological data, *Mol. Phylogen. Evol.*, 107, 308-323, 2017.
- 405 Ren, H., Lu, L.-M., Soejima, A., Luke, Q., Zhang, D.-X., Chen, Z.-D., and Wen, J.: Phylogenetic
406 analysis of the grape family (Vitaceae) based on the noncoding plastid trnC-petN, trnH-psbA, and
407 trnL-F sequences, *Taxon*, 60, 629-637, 2011.
- 408 Rix, M. G. and Harvey, M. S.: Phylogeny and historical biogeography of ancient assassin spiders
409 (Araneae: Archaeidae) in the Australian mesic zone: Evidence for Miocene speciation within Tertiary
410 refugia, *Mol. Phylogen. Evol.*, 62, 375-396, 2012.
- 411 Santos, M. F., Lucas, E., Sano, P. T., Buerki, S., Staggemeier, V. G., and Forest, F.: Biogeographical
412 patterns of *Myrcia* s.l. (Myrtaceae) and their correlation with geological and climatic history in the
413 Neotropics, *Mol. Phylogen. Evol.*, 108, 34-48, 2017.



- 414 Scurlock, J. M. O. and Hall, D. O.: The global carbon sink: a grassland perspective, *Glob. Chang. Biol.*,
415 4, 229-233, 1998.
- 416 Shafer, A. B. A. and Wolf, J. B. W.: Widespread evidence for incipient ecological speciation: a
417 meta-analysis of isolation-by-ecology, *Ecol. Lett.*, 16, 940-950, 2013.
- 418 Shen, C., Liu, K.-B., Morrill, C., Overpeck, J. T., Peng, J., and Tang, L.: Ecotone shift and major
419 droughts during the mid-late holocene in the central Tibetan Plateau, *Ecology*, 89, 1079-1088, 2008.
- 420 Sun, Y., Wang, A., Wan, D., Wang, Q., and Liu, J.: Rapid radiation of *Rheum* (Polygonaceae) and
421 parallel evolution of morphological traits, *Molecular Phylogenetics & Evolution*, 63, 150-158, 2012.
- 422 Tapponnier, P., Xu, Z. Q., Roger, F., Meyer, B., Arnaud, N., Wittlinger, G., and Yang, J. S.: Geology -
423 Oblique stepwise rise and growth of the Tibet plateau, *Science*, 294, 1671-1677, 2001.
- 424 Tedesco, P. A., Paradis, E., Leveque, C., and Hugueny, B.: Explaining global-scale diversification
425 patterns in actinopterygian fishes, *J. Biogeogr.*, 44, 773-783, 2017.
- 426 Thomasson, J. R.: Epidermal patterns of the lemma in some fossil and living grasses and their
427 phylogenetic significance, *Science*, 199, 975-977, 1978.
- 428 Turner, S., Hawkesworth, C., Liu, J., Rogers, N., Kelley, S., and Calsteren, P. V.: Timing of Tibetan
429 uplift constrained by analysis of volcanic rocks, *Nature*, 364, 50-54, 1993.
- 430 Voskamp, A., Baker, D. J., Stephens, P. A., Valdes, P. J., and Willis, S. G.: Global patterns in the
431 divergence between phylogenetic diversity and species richness in terrestrial birds, *J. Biogeogr.*, 44,
432 709-721, 2017.
- 433 Wang, G.-H., Li, H., Zhao, H.-W., and Zhang, W.-K.: Detecting climatically driven phylogenetic and
434 morphological divergence among spruce (*Picea*) species worldwide, *Biogeosciences*, 14, 2307-2319,
435 2017a.
- 436 Wang, P. X., Jian, Z. M., Zhao, Q. H., Li, Q. Y., Wang, R. J., Liu, Z. F., Wu, G. X., Shao, L., Wang, J.
437 L., Huang, B. Q., Fang, D. Y., Tian, J., Li, J. R., Li, X. H., Wei, G. J., Sun, X. J., Luo, Y. L., Su, X.,
438 Mao, S. Z., and Chen, M. H.: Evolution of the South China Sea and monsoon history revealed in
439 deep-sea records, *Chin. Sci. Bull.*, 48, 2549-2561, 2003.
- 440 Wang, X., Ma, X., and Yan, Y.: Effects of soil C:N:P stoichiometry on biomass allocation in the alpine
441 and arid steppe systems, *Ecology and Evolution*, 7, 1354-1362, 2017b.
- 442 Wang, Y., Cheng, H., Edwards, R. L., Kong, X., Shao, X., Chen, S., Wu, J., Jiang, X., Wang, X., and
443 An, Z.: Millennial- and orbital-scale changes in the East Asian monsoon over the past 224,000 years,
444 *Nature*, 451, 1090-1093, 2008.
- 445 Wu, J., Zhang, Q., Li, A., and Liang, C.: Historical landscape dynamics of Inner Mongolia: patterns,
446 drivers, and impacts, *Landscape Ecol.*, 30, 1579-1598, 2015.
- 447 Yuan, Z. Y., Jiao, F., Li, Y. H., and Kallenbach, R. L.: Anthropogenic disturbances are key to
448 maintaining the biodiversity of grasslands, *Sci. Rep.*, 6, 2016.
- 449
- 450
- 451
- 452
- 453
- 454
- 455



456

457 **Tables**458 **Table 1** Relevant information about samples used in the experiment. The latin name indicates

459 Stipa species latin name. The origin indicates the location of Stipa species. The altitude indicates

460 Stipa species altitude. The latitude and longitude indicates Stipa species latitude and longitude.

461 The area type indicates the partition type of Stipa species in RASP software.

Species name	Latin name	Origin	Altitude (m)	Latitude and longitude	Area type
<i>Stipa baicalensis</i>	<i>Stipa baicalensis</i>	Hulunbuir, Inner Mongolia	1650	49°20'57"N 120°07'09"E	A
<i>Stipa krylovii</i>	<i>Stipa krylovii</i>	Xilingol League, Inner Mongolia	930	47°51'58"N 115°46'48"E	B
<i>Stipa capillata</i>	<i>Stipa capillata</i>	Jungar Banner, Inner Mongolia	895	39°26'27.7"N 111°09'43.2"E	B
<i>Stipa grandis</i>	<i>Stipa grandis</i>	Xilingol League, Inner Mongolia	1686	44°30'25.9"N 117°21'47.1"E	B
<i>Stipa breviflora</i>	<i>Stipa breviflora</i>	Darhan Muminggan United Banner, Inner Mongolia	1376	41°50'18.1"N 110°13'45.3"E	B
<i>Stipa klemenzii</i>	<i>Stipa klemenzii</i>	Saihan Tala	1123	42°48'49.9"N 112°36'18.4"E	B
<i>Stipa glareosa</i>	<i>Stipa glareosa</i>	Erenhot, Inner Mongolia	942	43°36'42.2"N 111°59'29.9"E	B
<i>Stipa tianschanica</i>	<i>Stipa tianschanica</i>	Helan Mountains, Inner Mongolia	1715	38°42'49.5"N 105°58'43.7"E	C



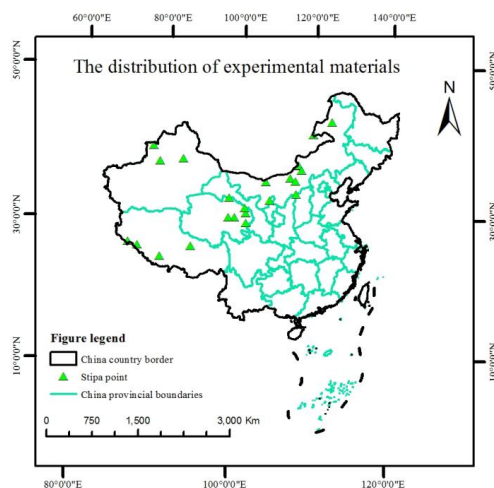
<i>Stipa aliena</i>	<i>Stipa aliena</i>	Qilian Mountains, Qinghai	3201	37°36'38.9"N 101°19'31.3"E	D
<i>Stipa penicillata</i>	<i>Stipa penicillata</i>	Haibei, Qinghai	3201	37°36'43.7"N 101°19'09.0"E	D
<i>Stipa regeliana</i>	<i>Stipa regeliana</i>	Haibei, Qinghai	3220	37°37'04.6"N 101°19'32.3"E	D
<i>Stipa przewalskyi</i>	<i>Stipa przewalskyi</i>	Haixi, Qinghai	2936	37°13'09.5"N 101°32'11.8"E	D
<i>Stipa purpurea</i>	<i>Stipa purpurea</i>	Haibei, Qinghai	3456	37°03'39.0"N 101°41'55.5"E	E
<i>Stipa orientalis</i>	<i>Stipa orientalis</i>	Nagqu, Tibet	4483	31°26'26.6"N 92°01'07.2"E	F
<i>Stipa roborowskyi</i>	<i>Stipa roborowskyi</i>	Tibet	4805	30°29'02.3"N 81°10'19.0"E	F
<i>Stipa subsessiliflora</i>	<i>Stipa subsessiliflora</i>	Tibet	3444	32°57'24.28"N 95°15'46.05"E	F
<i>Stipa capillacea</i>	<i>Stipa capillacea</i>	West Ngamring County, Tibet	4487	29°19'27.27"N 86°58'28.81"E	F
<i>Stipa capillacea</i>	<i>Stipa basiplumosa</i>	Tibet	4655	30°20'09"N 82°54'31.6"E	F
<i>Stipa caucasica</i>	<i>Stipa caucasica</i>	Sai Hubei, Xinjiang	2170	44°54'03.8"N 81°43'20.9"E	G
<i>Stipa sareptana</i>	<i>Stipa sareptana</i>	Xinjiang	1750	49°24'55.1"N 95°26'36.5"E	G
<i>Achnatherum splendens</i>	<i>Achnatherum splendens</i>	Xilamuren, Inner Mongolia	1607	41°20'48.5"N 111°10'17.0"E	B
<i>Ptilagrostis pelliottii</i>	<i>Ptilagrostis pelliottii</i>	Urad Middle Banner, Inner Mongolia	1518	41°53'36.8"N 107°43'32.2"E	B
<i>Helictotrichon</i>	<i>Helictotrichon</i>	Bayanbulak,	2470	42°54'0"N	G



schellianum *schellianum* Xinjiang 83°43'0"E

462

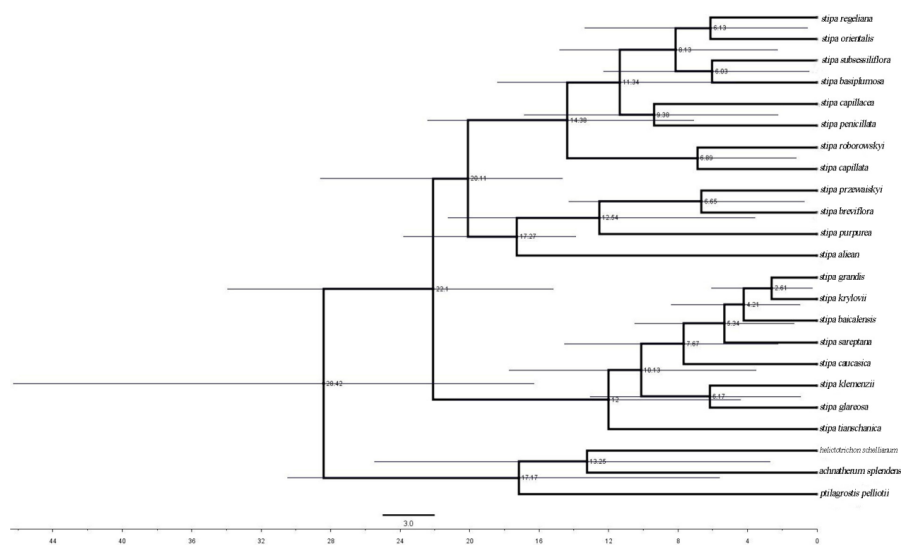
463 **Figure Legends**



464

465 **Figure 1** Distribution of sample material collection points. The green triangle means the
 466 distribution of *Stipa* species. The green line represents the China provincial boundaries. The black
 467 frame means China country borders.

468

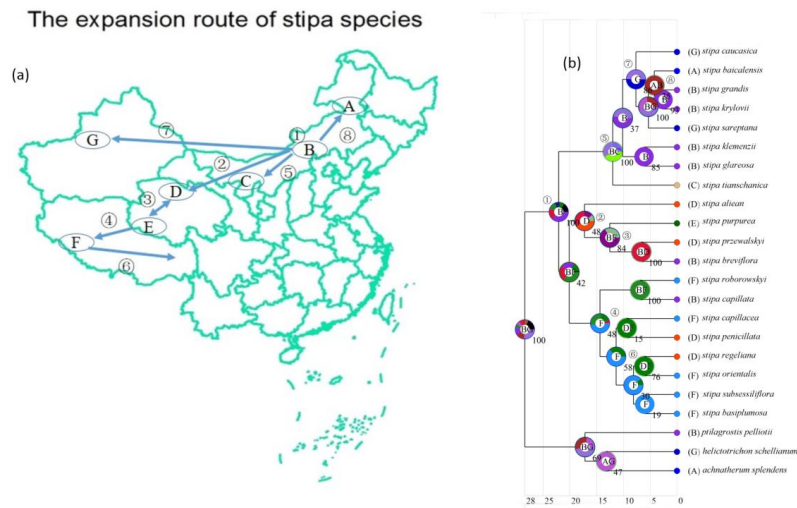


469

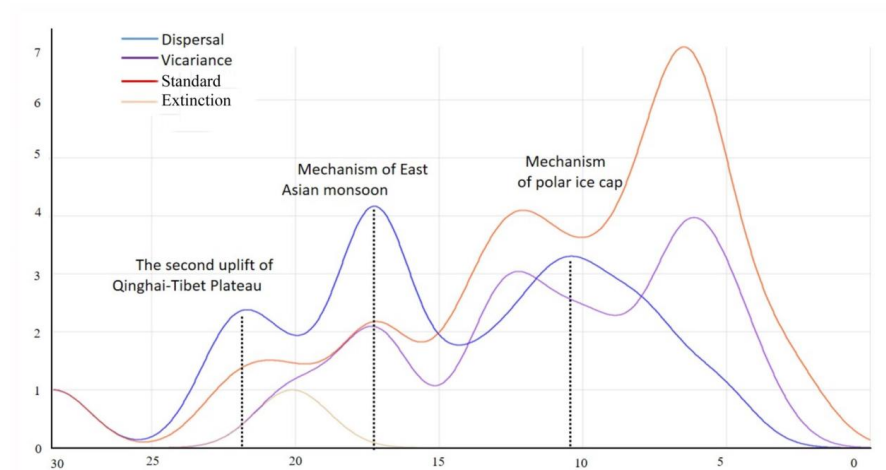
470 **Figure 2** Divergence time of *Stipa* species based on BEAST (Units: Ma, million years). The right



471 side of the picture is the Latin name of the *Stipa* species. The number of branches is the
 472 divergence time of *Stipa* species. 3.0 means the branch length of divergence time tree. The line
 473 segment represents time scale on the bottom of picture.
 474



475
 476
 477 **Figure 3** Analysis of ancestral geographic distribution of *Stipa* species using RASP. In figure 3(a),
 478 The Chinese grasslands were divided into seven sections: (A) eastern Inner Mongolia, (B) central
 479 Inner Mongolia, (C) the Helan Mountains, (D) the Qilian Mountains, (E) Qinghai, (F) Tibet, and
 480 (G) Xinjiang. The one-way arrows indicate the expansion route calculated using RASP, the
 481 two-way arrow indicates the phenomenon of mutual expansion between two areas. In figure 3(b),
 482 The right side of the picture is the Latin name of the *Stipa* species. The letter on each node of the
 483 tree represents the largest possible distribution area of *Stipa* species in the corresponding time
 484 period. The line segment represents time scale on the bottom of picture. ①-⑧ in Figs 3a and 3b
 485 are landmark nodes of the origin, divergence, and expansion of *Stipa* species.



486

487

488 **Figure 4** The time-geological time curve. The population dynamics of *Stipa* species was described
489 by time abscissas and range ordines. There are four curves in the graph, and the blue curve
490 represents the expansion trend of *Stipa* species, the purple curve represents the vicariance trend of
491 *Stipa* species, the pink curve represents extinction of *Stipa* species, the red curve is the standard
492 curve.